Identification of stable surfaces within point clouds for areal deformation monitoring

E. Friedli, A. Wieser

Institute of Geodesy and Photogrammetry (IGP),

ETH Zürich, Stefano-Franscini-Platz 5, 8093 Zürich, Switzerland

Abstract. Terrestrial laser scanning (TLS) allows acquiring the geometry of objects and surfaces with high spatial resolution and high accuracy over large areas. So, it is a potentially attractive technology for structural monitoring and geomonitoring. For these purposes a sequence of scans has to be acquired at different epochs, and changes between the epochs need to be detected and quantified by analyzing the resulting point clouds. An essential step in this analysis is the transformation of the point clouds into a common, stable reference system. Standard approaches, well established for other purposes of TLS, are not applicable or not sufficiently accurate for monitoring if long scanning distances arise (several hundred meters or more) or significant parts of the point cloud change between the scan acquisitions.

We present an approach for a data driven registration of pairs of scans, which can easily be extended to entire scan sequences. The core of the approach is the automatic identification of stable areas and their use for the fine registration. This is achieved through an iterated segmentation of the point clouds into stable and unstable parts based on octree cells and distances between centroids. The process is repeated until the transformation obtained using ICP does not change significantly anymore between consecutive iterations.

The proposed approach and the resulting extraction of deformations are successfully demonstrated using two data sets with very different characteristics: (i) an indoor scene (close range, controlled environment) and (ii) an alpine glacier (long distance, real monitoring application). The results show that the algorithm is working well if certain control parameters have been chosen sensibly.

Keywords. Terrestrial laser scanning, change detection, geodetic monitoring, datum realization, registration.

1 Introduction

The core task of geodetic deformation monitoring is the statistically founded identification and quantification of geometric changes with respect to a stable reference frame. This reference frame can be based on points known to be stable and located outside or within the monitored area. In the former case the reference frame is typically realized using GNSS. In the latter case, several difficulties arise. First, it may not be clear beforehand which points are actually stable and which are not; thus the definition of the geodetic datum by classification of monitored points as either stable (reference points) or unstable (object points) is an integral component of classical, strict deformation analysis, see e.g. Niemeier (1985), Caspary (2000), Heunecke et al. (2014). Secondly, the sensors used for monitoring may not be appropriate for identifying individual, clearly defined points at all, and thus the stable reference frame needs to be realized using different means. This is the case in particular for terrestrial laser scanning (TLS), and the datum realization problem is not yet solved satisfactorily for TLS-based monitoring.

A well-established standard solution for registering various laser scans i.e., for transforming them into a common coordinate system, is to place artificial objects (e.g., spheres or retroreflective targets) within the scanned scene, identify them in the different scans during post-processing, estimate a representative point (e.g., the center) for each of them from the coordinates and possibly signal-strengths within the TLS point cloud, and finally use these points to estimate the parameters of a congruency transformation between the individual point clouds. These point clouds can either be obtained by scanning from different locations at one monitoring epoch (i.e., assuming the monitored scene to be stable while these scans are taken) or by scanning at different epochs (assuming that potential changes occurred between these). For transforming the point clouds into an external reference frame the positions

of some of these artificial objects need to be determined separately e.g., using GNSS or a total station (Barbarella et al., 2013; Prokop & Panholzer, 2009; Bitelli et al., 2004). It is possible to obtain the georeferencing data simultaneously with the point clouds by integrating a GNSS antenna into the targets (spheres) and collecting GNSS data while scanning.[1] This idea can be extended to cases where the targets move between scanning epochs, and could even allow quasi-continuous monitoring by fully automatic repeated scanning.

However, placing the targets may be cumbersome or hardly possible for a monitoring application (area of interest might be inaccessible or access may be dangerous), and assuring their stability with respect to the immediate neighborhood may require significant in-situ work (e.g. for setting up a pillar). Even more critically, the laser scanner will have to be set up in one or more safe locations with sufficiently unobstructed view to sufficiently large parts of the area of interest. For quasi-continuous monitoring, the setup location will additionally have to be stable. So, the instrument location(s) will typically be far from the monitored surfaces (several hundred meters or more). At such distances, spheres and other artificial targets of manageable size (a few cm to dm of diameter) are too small in relation to the footprint and angular increment of the scanner for reliable detection and accurate estimation of the respective center. For reasons of uncertainty propagation the targets cannot be located much closer than the monitored surfaces.

Solutions that avoid the need of artificial targets are of great interest therefore. Such solutions exploit the potentially high redundancy provided by the large number of points within the point cloud and are typically either based on the iterative closest point (ICP) algorithm, Besl and McKay (1992), Chen and Medioni (1992), or on automatic extraction and correspondence detection of geometric features, e.g., planes, within the point clouds, see Previtali et al. (2014) for a recent overview with many further references. These registration algorithms work well if there are no or only negligible geometric changes between the overlapping point clouds. This is in contrast to what we expect when applying point cloud based technologies to deformation monitoring, where a significant part of the point cloud may change between epochs.

We are working on an approach for areal deformation monitoring using point clouds which automatically detects stable and unstable regions within the point cloud, and ultimately represents deformations and changes based on identifying objects and distinct surface patches within the instable parts, using the stable parts of the point cloud for datum realization. In this paper, we focus on the proposed algorithm for automatically identifying the stable regions within two point clouds covering approximately the same area and obtained at different epochs. The approach can easily be extended to a time series of point clouds by pairwise application to consecutive epochs or to a reference and a monitoring epoch.

The algorithm consists of an iterated segmentation of the two point clouds into a part with points transforming equally (supposed to be the stable part) and parts with points transforming differently (supposed to be the instable parts). Similar to the approach in Wujanz et al. (2014) octree cells are used to partition the point clouds. The segmentation is preceded by a coarse alignment of the point clouds, and it is followed by a transformation of both point clouds into a common coordinate systems represented by the entirety of the points classified as stable. Finally, the changes between the two epochs are analyzed using only the points classified as unstable.

The algorithm is presented in sec. 2. Its application to real data sets is demonstrated and discussed in sec. 3.

2 Methods

2.1 Coarse Alignment

We assume that the entire area to be monitored is covered by a single point cloud per epoch, and that point clouds for the two epochs t_i and t_j are available. First the two point clouds need to be coarsely aligned by transforming them approximately into the same coordinate system. This can be achieved automatically, e.g., using the Keypoint-based 4-Points Congruent Sets (K-4PCS) method proposed by Theiler et al. (2014). It can also be achieved manually using the corresponding tools within standard point cloud processing software.

If scanning from one location is enough and the scanner is permanently installed (e.g., on a pillar) with sufficiently stable orientation, the coarse

---

[1] Glira et al. (2013) have investigated this based on a proposal by the second author of the present paper.

alignment is already achieved through this stable setup.

2.2 Segmentation and Registration

Both point clouds are then split into equally sized octree cells (Meagher, 1992) by using the same resolution S_{min} corresponding to the size of voxels at the lowest octree level. S_{min} is chosen by the user under consideration of the point density within the point cloud (sufficient number of points within each cell containing relevant parts of the monitored area) and the size of objects possibly moving or changing shape within the area of interest (ideally no more than one such object per cell). For instance, $S_{min} = 5$ cm was chosen for the data set shown in Fig. 1.
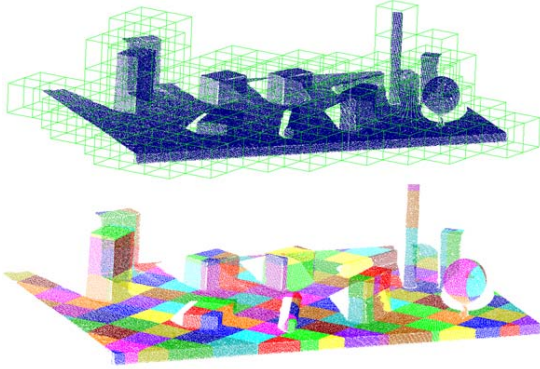

Fig. 1 Example of an octree based point cloud segmentation with a resolution $S_{min} = 10$ cm (top: wireframe with input cloud; bottom: points colored in correspondence with the cell they belong to).

Ignoring the fact that the two point clouds have been aligned only approximately, they are split using perfectly identical octree cells (i.e., equal coordinates of corresponding corners). We have enforced this in our software implementation, based on the point cloud library (PCL)[2], by specifying an identical bounding box for both point clouds in addition to using the same value S_{min}. The bounding box is calculated such that it actually contains all points of both point clouds.

Each octree cell containing less than a minimum number N_{min} of points is subsequently ignored, i.e., the points within such cells are not used during the current iteration of the algorithm. This mitigates the effect of spurious points and eventual outliers (e.g.,

---

[2] http://pointclouds.org

points in the air). In the numeric examples below, we have used $N_{min} = 20$.

Now the points within a certain octree cell $C_{k,i}$ for epoch t_i need to be associated with the corresponding points of epoch t_j. We assume that these corresponding points are again within one octree cell, and search for that cell $C_{k,j}$ in the neighborhood of $C_{k,i}$. We do this by calculating the geometric centre (centroid) of all octree cells from the respective inlying points and carrying out a k-d tree based search (Bentley, 1975) to find the nearest centroid in the cloud of t_j for each centroid in the cloud of t_i. The result is a pairwise association of octree cells (one obtains pairs of centroids for corresponding octree cells in a temporal sequence of scans).
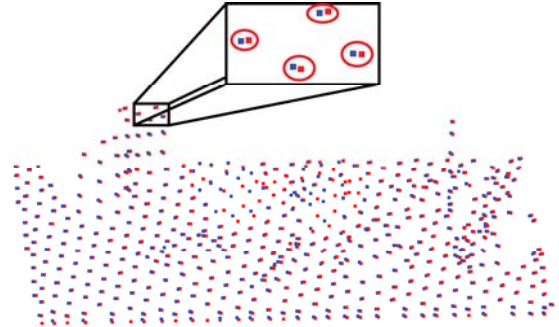

Fig. 2 Centroids of the octree cells of two scan epochs. Red points belong to the first and blue points to the second acquisition. The 3D distances of the centroid pairs (marked with red ellipses) are between 3.8 and 4.2 mm.

Now the difference vectors of the centroids of the corresponding cells are calculated. Based on this information, a classification into stable (no change occurred) and unstable (something has happened) is made. If the coordinate difference of a pair of centroids stays within a given threshold (D_{max}), it is assumed that the octree cells are identical, and therefore no deformation has occurred. These cells are then classified as stable. This D_{max} can either be data based or on prior knowledge. Both of them can have their justification depending on the situation that is observed.

$$\left\| \overline{X}_{k,i} - \overline{X}_{k,j} \right\| := D_{k,i,j} \le (\overline{D}_{i,j} + s_{D_{i,j}}) \qquad (1)$$

$$\left\| \overline{X}_{k,i} - \overline{X}_{k,j} \right\| := D_{k,i,j} \le (\tilde{D}_{i,j} + 1.483 \cdot \tilde{a}_{D_{i,j}}) \qquad (2)$$

$$\left\| \overline{X}_{k,i} - \overline{X}_{k,j} \right\| := D_{k,i,j} \le D_{max} \qquad (3)$$

with

$\overline{X}_{k,i}$ centroid of octree cell k in epoch i

$\overline{D}_{i,j}$ average distance of all corresponding octree cells between epochs i and j

$s_{D_{i,j}}$ empirical standard deviation of these distances

$\tilde{D}_{i,j}$ median of these distances

$\tilde{a}_{D_{i,j}}$ median of their absolute deviations (MAD)

D_{max} user selected threshold

For scans where the majority of points refer to stable areas we found the data based thresholds as in (1) and particularly the more robust version (2) to work well. However, they both failed in cases where more than 50% of the points were associated with moving areas. In this case, a user selected value D_{max} reflecting the accuracy of the approximate alignment, the accuracy of the scanner, and the roughness of the stable surfaces within the octree cells is suitable to correctly identify stable areas.

All points belonging to cells classified as stable are then transformed from epoch t_j to t_i by fine registration using ICP. The resulting transformation parameters are applied to the entire point cloud of epoch t_j.

For control purposes, the bounding box is also transformed using the same parameters. If the approximate alignment (as described in sec. 2.1) was sufficiently accurate, the coordinates of the bounding box points will not change significantly by this transformation. If they do, the result obtained so far is considered a better approximation of the alignment between the two epochs, and the entire process described in sec. 2.2 is repeated starting from that approximation. This is carried out iteratively until convergence is achieved i.e., the coordinates of the bounding box do not change significantly by the transformation. Now the points of both epochs are available in the same coordinate frame (defined by the stable areas of t_i) and deformation analysis can be carried out.

2.3 Deformation Analysis

Once the datum has been established using the points associated with stable parts of the monitored area, the deformations/changes in the other parts can be analyzed. This is the last step of the workflow, and its investigation is the subject of future work. We have chosen two different approaches to analyze the changes in the numeric examples within this paper. One is to derive displacement vectors between the surfaces by using directly the points within the point cloud, or the triangular mesh derived therefrom. For this approach we use the "3D compare" tool in Geomagic[3]. The tool calculates and visualizes the distance between the mesh of t_i and t_j pointwise either along fixed, predefined directions (e.g. vertical) or along the respective direction of least distance, which varies depending on location and topography of the surfaces. The results of such an analysis are easy to calculate but may be very difficult to interpret in particular with respect to object displacement and rotation.

A useful alternative approach would be to identify objects within the unstable areas, analyze the rigid body motion and deformation of these objects, and the deformation of the background. Since this is subject of future work, we have chosen a much simpler alternative approach, based on using the centroids within the unstable areas as feature points.

Assuming that the correspondence between two centroids of unstable cells is correct, we obtain the translation of a known point and not just a difference between two surfaces where we cannot track a single point as with the first method presented. However, this approach delivers only meaningful results if the points within a cell move similarly and no rotation occurred. To overcome this problem, the translations of a set of neighboring centroids could be used.

3 Application examples

Two different data sets are used to test the algorithms presented above using parts of PCL for their implementation. The first one is a short-range indoor scene with a couple of small objects of regular and simple geometry arranged on a table (Fig. 3) and scanned using a Faro Focus[3D] S 120 from a distance of about 2 m. Changes were introduced by manually moving two of the cuboids. This data set represents a highly controlled situation with known ground truth and negligible environmental impacts.

The second data set consists of two scans of the Weissmies glacier (Fig. 4) in Valais, Switzerland, acquired in April and September 2015 from a dis-

---

[3] http://www.geomagic.com/en/

tance of about 1.5 km using a Riegl VZ-6000. For this data set representing a real monitoring application ground truth is not available. However, plausibility checks can be performed on the results using displacement rates from terrestrial radar interferometry obtained during the entire period between the two scans.
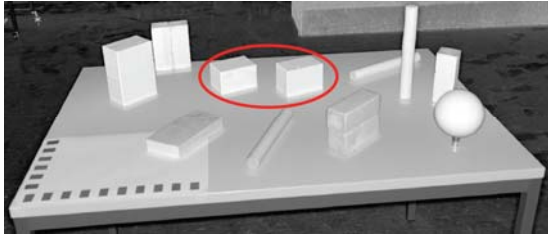

Fig. 3 Image of indoor scene with the two moved cuboids (red ellipse). The size of the table is 120×80 cm^2

Fig. 4 Image of the scanned area $(1000 \times 800 \text{ m}^2)$ at the Weissmies glacier.

3.1 Results of indoor data set

Fig. 5 shows the result of the classification obtained using $S_{min} = 5$ cm and the data driven distance threshold of eq. (1). Corresponding to the true situation, most octree cells were classified as stable in this case. Potential false positives (cells classified as unstable although they contain in reality only points associated with stable areas) are not a problem at this stage, because the corresponding points are just omitted for the datum definition, and there are still by far enough points left for an accurate registration of the two epochs. In fact, the classification result shows that the fine registration of the indoor scans is based only on points that did not move.

If we have a closer look at the area surrounding the two moved cuboids (Fig. 6), which is also the only area where cells were classified as unstable, we see that false positives only occurred at a few places on the table behind the cuboids. These false classifications are due to the different obstruction of the background by the moved cuboids. After the cuboids have been shifted more of the table be-

comes visible in the background to the left of the objects, while more of it becomes obstructed to the right of them. Correspondingly, the centroids of octree cells containing partially shaded parts of the table are shifted as the obstruction changes. Similar effects would have to be expected in many parts of the scene if the scanner location changed between epochs. However, this is not critical as long as it does not cause a significant number of false negatives i.e., many actually unstable areas to be classified as stable and thus deteriorating the quality of the registration.
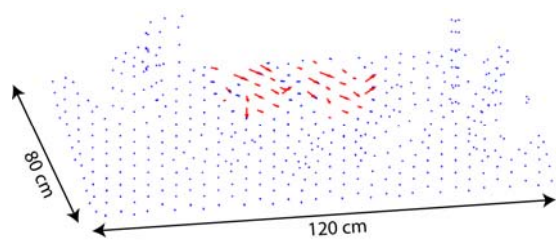

Fig. 5 Classification result for the indoor scene. The arrows represent the displacement vectors of the centroids (red for cells classified as unstable, blue for cells classified as stable).
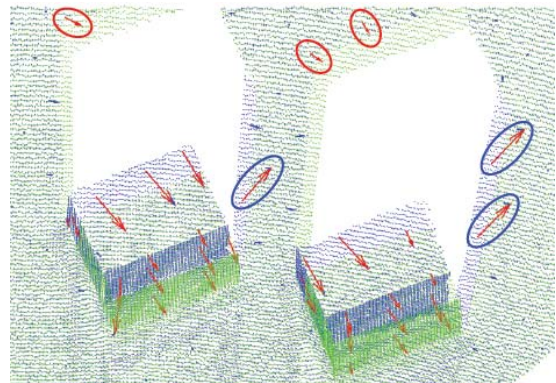

Fig. 6 Display of the two point clouds overlaid with the displacement vectors of the centroids. Blue points represent the first acquisition, green points the second one. The red arrows show the displacement of cells classified as unstable, the ellipses indicate false detections due to decreasing (red) or increasing (blue) obstruction.

Finally, the surface deviations between the clouds were calculated using the Geomagic tool mentioned in sec. 2.3. To highlight the quality of the registration, these deviations are shown for the entire scene in Fig. 7, not only for the areas classified as unstable. The figure shows that the differences are below

5

1 mm almost everywhere within the stable areas (compare to Fig. 5); this indicates the successful registration. The cuboids were moved by 25 mm, and this is very well reflected in terms of magnitude by the extracted surface differences. If the information from the difference vectors (Fig. 5 and Fig. 6) of the centroids is taken into account too, the direction of the movement can also be estimated.
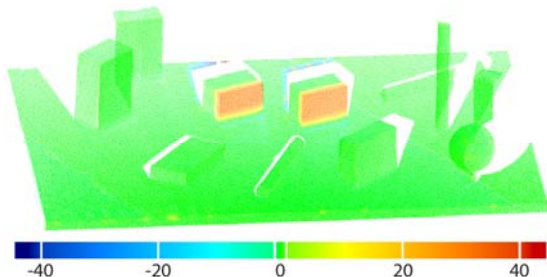

Fig. 7 Deviations (in mm) of the point clouds of the indoor data set after the proposed fine registration; deviations obtained using the "3D Compare" tool in Geomagic.

Further investigations will be devoted to the appropriate, possibly adaptive, choice of S_{min}. The associated problem can easily be visualized using the indoor data set. If S_{min} is too large there may be little or no cells only containing points from moved areas, and such points will have too little influence in mixed cells which will consequently be classified as stable. If, on the other hand, S_{min} is too small objects can move from one cell into another one, and false correspondences may be selected as displayed in Fig. 8.
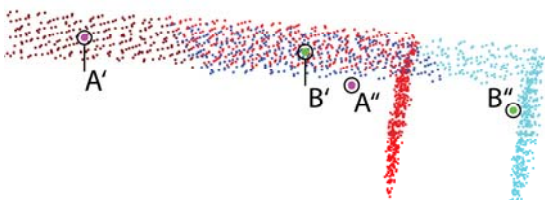

Fig. 8 Example of falsely matched cells. Cell B' was matched to A" instead of B", because of too small S_{min}.

3.2 Results of outdoor data set

The influence of the D_{max} is demonstrated with the example of the Weissmies glacier where more most of the scanned area is moving. As mentioned before, this threshold is used to classify the cells into stable and unstable depending on whether the limit is exceeded or not.

Using the (robust) data driven distance threshold of eq. (2), most of the areas covered by the scans of the Weissmies glacier are classified as stable (Fig. 9, top). However, from interferometric radar data we know that the glacier is actually moving, and thus the majority of the points in the point cloud should be classified as unstable. The data driven selection of the threshold fails, because most of the scene is moving. Taking into account the expected scanning accuracy, we therefore chose a fixed threshold of 10 cm according to eq. (3). A comparison of the classification result (Fig. 9, bottom) to the image of the glacier (Fig. 4) shows that the points now classified as stable are actually located on the rock faces, which are indeed expected to be stable, whereas most of the glacier surface was correctly classified as unstable. The algorithm again seems to be successful.
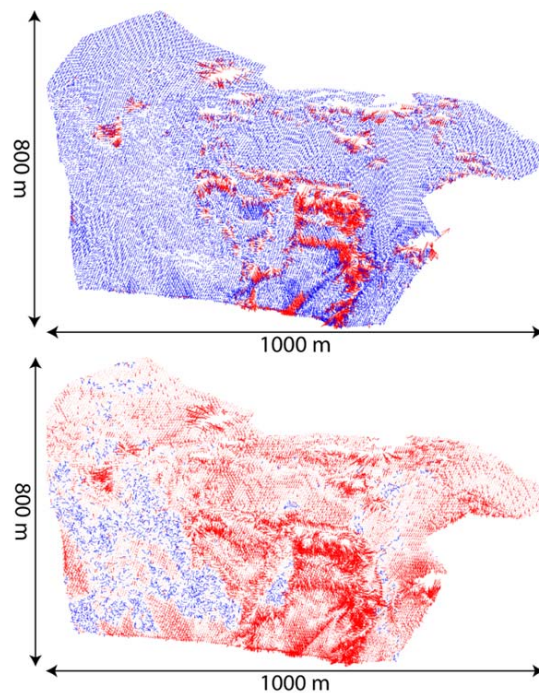

Fig. 9 Results of the classification with different displacement thresholds (eq. (2), top; $D_{max} = 10$ cm, bottom). The arrows symbolize the shift of the centroid for each octree cell. Blue arrows denote stable cells, red unstable ones, according to the classification.

The visualization of the differences between the two registered point clouds (Fig. 10) supports this assumption. The rocky areas show no significant

6

changes (displacements < 10 cm) and there seems to be no rotation left despite the fact that most stable points are concentrated in the left part of the point cloud. The order of magnitude of the other changes is plausible and can be attributed to glacier flow, ice break-offs, melting and similar processes. As with the indoor scene, one can analyze the changes in combination with the result of the difference vectors shown on the bottom image of Fig. 9.
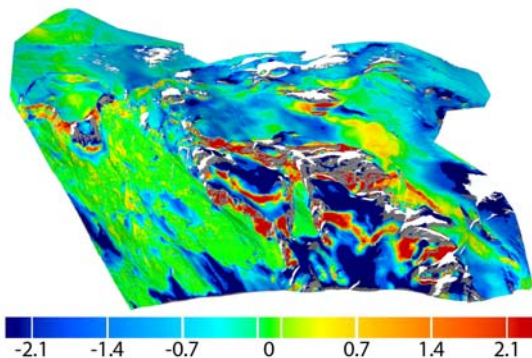

Fig. 10 Deviations (in m) of the point clouds of the Weissmies glacier after the proposed fine registration; deviations calculated using the "3D Compare" tool in Geomagic.

4 Conclusion

In this paper we presented a marker less approach to register point clouds for monitoring based on terrestrial laser scanning. The goal of the proposed approach is to transform the scans of all epochs into a common, stable reference frame. This is achieved by iterative segmentation of pairs of point clouds into stable and unstable parts, and fine registration using ICP based on the stable parts only. Two parameters control the performance of the resulting algorithm, the minimum size of the octree cells used for partitioning the point clouds, and the maximum calculated displacement with which parts of the point clouds are classified as stable. Although a data driven approach has been presented and successfully used, further investigations are required to adaptively and optimally determine these parameters.

We have successfully demonstrated the proposed approach using (i) an indoor scene where the known displacement of 25 mm of two objects was correctly indicated by the results, and (ii) an outdoor scene where the changes of a glacier during the 6 months between the scans were plausibly indicated. Future work will be focused on extending the approach to a more comprehensive, object based analysis of the unstable areas.

References

Barbarella, M., M. Fiani and A. Lugli (2013). Landslide monitoring using multitemporal terrestrial laser scanning for ground displacement analysis. In: *Geomatics, Natural Hazards and Risk*, Vol. 6, No. 5-7, pp. 398-418

Bentley J.L. (1975). Multidimensional binary search trees used for associative searching. In: *Commun. ACM*, Vol. 18, No. 9, pp. 509-517.

Besl, P.J. and N.B. McKay (1992). A method for registration of 3-D shapes. In: *IEEE Transactions on Pattern Analysis and Machine Intelligence*, Vol. 14, No. 2, pp. 239-256.

Bitelli, G., M. Dubbini, and A. Zanutta (2004). Terrestrial laser scanning and digital photogrammetry techniques to monitor landslide bodies. In: *International Archives of Photogrammetry, Remote Sensing and Spatial Information Sciences*, Vol. 35, No. Part B 5, pp. 246-251.

Caspary, W.F. (1987). *Concepts of network and deformation analysis*, (Vol. 11). J. M. Rüeger (Ed.), Australia, University of New South Wales.

Chen, Y. and G. Medioni (1992). Object modeling by registration of multiple range images. In: *Image and Vision Computing*, Vol. 10, No. 3, pp. 145-155.

Glira P., C. Briese, N. Kamp, N. Pfeifer (2013). Simultaneous relative and absolute orientation of point clouds with "TLS radomes" In: *Geophysical Research Abstracts*, Vol. 15, p.13116.

Heunecke, O., H. Kuhlmann, W. Welsch, A. Eichhorn, H. Neuner (2013). *Auswertung geodätischer Überwachungsmessungen*, 2. Auflage, Wichmann-Verlag, (in German).

Meagher, D. (1982). Geometric Modeling Using Octree Encoding. In: *Computer Graphics and Image Processing*, Vol. 19, No. 2, pp. 129-147.

Niemeier, W. (1985). Deformationsanalyse. In: Pelzer H. (Ed.),*Geodätische Netze und in Landes- und Ingenieurvermessung*, Wittwer Verlag, (in German).

Previtali, M., L. Barazzetti, R. Brumana, M. Scaioni (2014). Laser scan registration using planar features. In: *ISPRS Archives*, Vol. XL-5, pp. 501-508.

Prokop, A. and H. Panholzer (2009). Assessing the capability of terrestrial laser scanning for monitoring slow moving landslides. In: *Natural Hazards and Earth System Sciences*, Vol. 9, No. 6, pp. 1921-1928.

Theiler, P.W., J.D. Wegner, and K. Schindler (2014) Keypoint-based 4-Points Congruent Sets – Automated markerless registration of laser scans. In: *ISPRS Journal of Photogrammetry and Remote Sensing*, Vol 96, pp 149 – 163.

Wujanz, D., D. Krueger and F. Neitzel (2014). Der ICProx-Algorithmus – oberflächenbasierte Registrierung terrestrischer Laserscans für die Deformationsanalyse. In: Wieser A. (Ed.), *Beiträge zum 17. Internationalen Ingenieurvermessungskurs*, Wichmann Verlag, pp. 245-256 (in German).